Multi-Sectioned Predictive Model of Cable Insulation under Reaction- and Diffusion-Controlled Degradation

Yuan-Shang Chang and Ali Mosleh
B. John Garrick Institute for the Risk Sciences, and Department of Materials Science & Engineering
University of California, Los Angeles (UCLA), USA

Abstract: Cable insulation is essential for power plants. It degrades due to thermal energy. The degradation of cable insulation can cause safety issues. Oxidation is one of the major reactions rendering the degradation. The antioxidant has been always added to the insulation to slow down the oxidation. In this paper, Bayesian Parameter Estimation is applied to model the uncertainty of the depletion process of the antioxidant. With respect to specific antioxidant content left in the insulation during aging, the trends of the Elongation at Break (EAB) have been modeled by discrete drop-off rates. Therefore, multi-sectioned EAB curves can be plotted according to each drop-off rate. With the uncertainty of the antioxidant content and the EAB curves, the time to failure of the insulation becomes a probabilistic representation. This approach is the first in the related research domain. Experimental data have been incorporated to validate the proposed models.

Keywords: Elongation at Break (EAB), insulation degradation, Bayesian parameter estimation, antioxidant.

1. INTRODUCTION

Cables are essential for power plants and the degradation of the cable insulation can be a safety issue. The degradation is usually characterized by Elongation at Break (EAB) [1-3]. Oxidation is a major reaction causing the degradation [4]. The antioxidant is always added to the insulation to slow down the oxidation [5]. The content of the antioxidant decreases during an aging process, which accelerates the degradation [5, 6]. Therefore, the degradation rate of the insulation with respect to the level of the antioxidant left in the insulation becomes an important topic.

For the oxidation reaction to occur, oxygen must diffuse from the surface into the insulation matrix. The second step is to overcome the activation energy of the reaction at the interface between the reactants: oxygen and polymer molecules. Both of the steps require time. The role of the antioxidant is to control the probability of a successful reaction constituted by the reactants [4]. When the concentration of the antioxidant is higher, the bottleneck of the oxidation reaction is the second step. In other words, the control step is the reaction rate at the interface rather than the diffusion rate of oxygen. On the contrary, while the antioxidant is deficient, the reaction rate at the interface becomes so high that the supply rate of oxygen is the critical step. To draw a line between the two controlling mechanisms, the depletion process of the antioxidant shall be investigated.

The oxidation rate and the drop-off rate of the EAB are higher when the antioxidant concentration becomes lower [5, 6]. In the previous study, the depletion of the antioxidant against time had been linearly modeled [5, 6]. Compared to the linear model, in this paper, the depletion process of the antioxidant is quantified by an exponential function, which is demonstrated more pertinent to the long-term prediction. Bayesian Parameter Estimation is applied to represent the depletion rate of the antioxidant with uncertainty. With the uncertainty of the depletion rate and the discrete drop-off rates of the EAB curve, the reliability of the insulation can be defined. This approach is first proposed in the related research domain and experimental data are incorporated to validate this approach.

2. MODELING

The concentration of the antioxidant in cable insulation can significantly affect the degradation rate of the insulation [6, 7]. Figure 1 is a schematic illustration representing the relation between the concentration and the degradation rate. The continuous line in Figure 1 (a) is plotted by equation (1) to model the experimental data denoted by the circles. y is the remaining antioxidant in the insulation. λ is depletion rate in [/hour]. t is time. τ_s is the time that is required to reach steady-state degradation with respect to λ.

The initial content of the antioxidant is c_1. While the content is above c_2 before t_1, the drop-off rate of the EAB is negligible, as shown by the incubation section in Figure 1 (b). The discrete lines composed of the dotted, dashed, and solid segments can all be represented by equation (2) and equation (3) derived from Dichotomy Model [8-10]. δ is normalized EAB. V_d is degradation ratio. ν is drop-off rate in [/hour]. τ_0 is incubation time. The drop-off rate of each segment is assumed constant and different from one another.
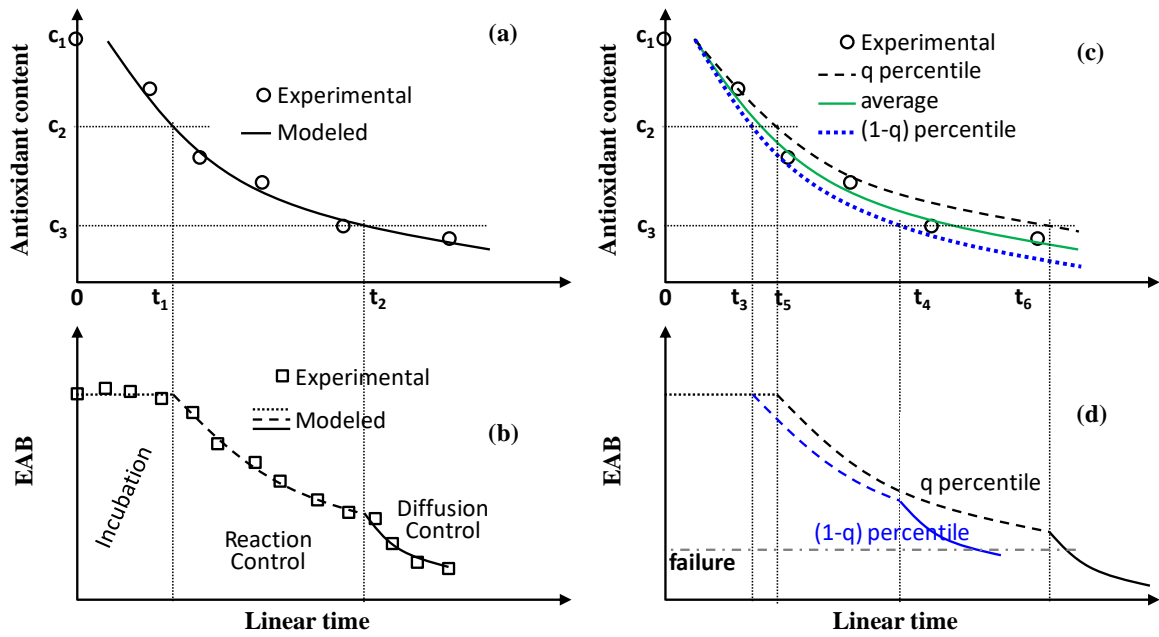

Figure 1. (a) Experimental (the circles) and fitted (the line) content of antioxidant. (b) The trend of the EAB corresponding to the content of the antioxidant. (c) The exponential fit of the content of the antioxidant. (d) The uncertainty of the EAB corresponding to the uncertainty of the content of the antioxidant.

$$y = e^{-\lambda(t-\tau_s)} \tag{1}$$

$$\delta \cong 1 - (V_d)^{(1/3)} \tag{2}$$

$$V_d = 1 - e^{-\nu(t-\tau_0)} \tag{3}$$

The experimental data in Figure 1 (a) and Figure 1 (c) are the same. However, Figure 1 (a) shows there is always uncertainty between the predicted and experimental values. Therefore, Bayesian Parameter Estimation [11-15], represented by equation (4), can be applied to model the uncertainty of the antioxidant during aging, which is shown by the lines in Figure 1 (c). The "data" in equation (4) are the experimental points in Figure 1 (c). In equation (5), y_i is the measured content of the antioxidant and assumed to be normally distributed with respect to a predicted value represented by μ_y where σ is the standard deviation of the normal distribution in equation (6). μ_y can be calculated by equation (1) and represented by equation (7). By plugging equation (7) into equation (6), equation (8) is obtained where t_i is a measured value of the aging time. Equation (8) serves as the likelihood function of equation (4).

$$\Pr(\theta \mid \text{data}) = \frac{\Pr(\text{data} \mid \theta)\,\Pr(\theta)}{\int \Pr(\text{data} \mid \theta)\,\Pr(\theta)d\theta} \qquad (4)$$

$$y_i \sim \mathcal{N}(\mu_y, \sigma) \qquad (5)$$

$$\Pr\left(y_i \mid \mu_y, \sigma\right) = \frac{1}{\sqrt{2\pi\sigma^2}} \exp\left(-\frac{\left(y_i - \mu_y\right)^2}{2\sigma^2}\right) \qquad (6)$$

$$\mu_y = e^{-\lambda(t - \tau_s)} \qquad (7)$$

$$\Pr(y_i, t_i \mid \lambda, \sigma) = \frac{1}{\sqrt{2\pi\sigma^2}} \exp\left(-\frac{\left(y_i - e^{-\lambda(t_i - \tau_s)}\right)^2}{2\sigma^2}\right) \qquad (8)$$

Based on equation (8) and equation (4) with the priors, λ and σ, the deterministic line in Figure 1 (a) becomes a probabilistic band represented by the dashed, solid, and dotted lines in Figure 1 (c). The same to the approach addressing the sections of the EAB in Figure 1 (b) corresponding to the content of the antioxidant in Figure 1 (a), Figure 1 (c) can render the uncertainty of the three sections, which is plotted in Figure 1 (d). The chained line is the acceptable minimum of the EAB. The intersection of the chained line and the band can define the reliability of the cable insulation. The models discussed above will be validated by experimental data in the following section.

3. VALIDATION

3.1. Drop-off Rate of the EAB

The experimental data for validation are from a published paper [6]. The antioxidant in XLPE is Nocrac-MB at the concentration: 0, 0.1, and 1 phr, which are labeled by 1A, 2A, and 3A, respectively. These samples are thermally aged at 135°C and their degradation of the EAB is plotted in Figure 2. By applying curve fitting, equation (2) and equation (3) can model the experimental data where τ_0 is assumed to be zero and the determined values of ν are listed in Table 1.
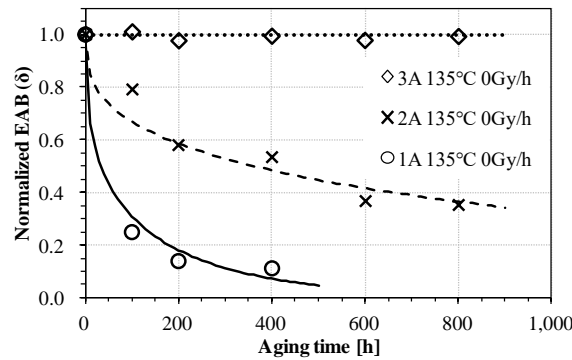

Figure 2. Comparison between experimental (discrete patterns) and modeled (continuous lines) EAB

Table 1. Modelled drop-off rate (ν)

Label		[$\times 10^{-4}$/hour]
1A	ν_1	40
2A	ν_2	3.7
3A	ν_3	~ 0

3.2. Depletion Rate of the Antioxidant

The depletion of Nocrac-MB in XLPE at 135°C thermal aging is plotted in Figure 3. To model the circles, equation (8) with Bayesian Parameter Estimation is applied. τ_s is assumed to be 100 hours. The priors, λ and σ, are assumed to be uniform distribution between 0-0.003 and 0-0.2, respectively. The results of λ and σ calculated by Bayesian Parameter Estimation are plotted by the PDFs in Figure 4 and Figure 5. The percentile of several λ values is listed in Table 2 and plotted in Figure 3. Corresponding to each λ value, the time required to reach a specific y value can be calculated by equation (1). The result is listed in Table 3.
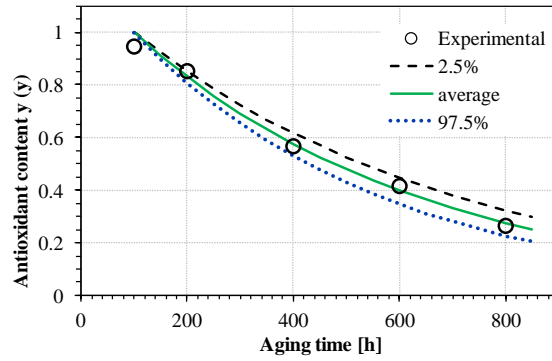

Figure 3. Comparison between experimental (the circles) and exponentially-modeled (the lines) antioxidant content
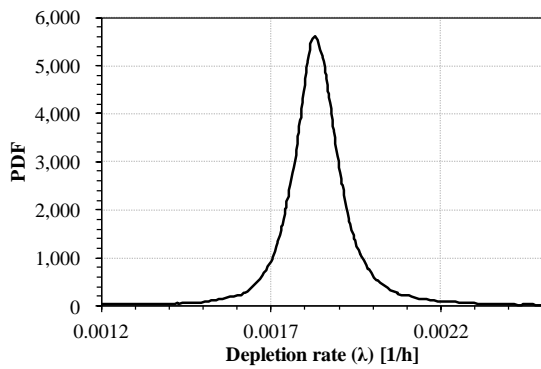

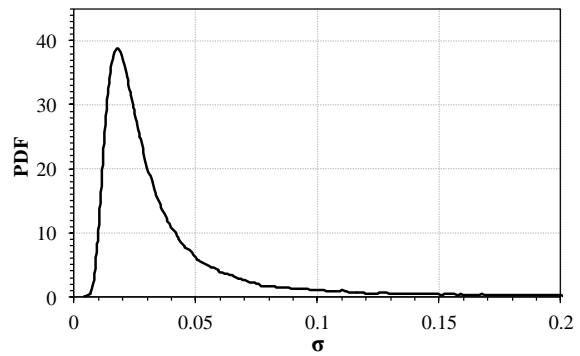Figure 4. PDF of the depletion rate of the antioxidant

Figure 5. PDF of the standard deviation

Table 2. The result of Bayesian parameter estimation

Percentile	$\lambda = [1/h]$
2.5	0.001615
25	0.001785
50*	0.001834
75	0.001886
97.5	0.002123

*The average of λ is 0.001841.

Table 3. The content of the antioxidant (y) vs. aging time (t_i) [hours]

Percentile of λ	$(t_1 - 0)$ $y = 0.1 = c_2$	$(t_2 - 0)$ $y = 0.02 = c_3$	$(t_2) - (t_1)$
2.5	1,526	2,522	997
Average	1,351	2,225	874
97.5	1,185	1,943	758

Figure 3 validated Figure 1 (c). To validate Figure 1 (d), Figure 6 is plotted. When the content of the antioxidant is higher than ($c_2 = 0.1$), or the aging time is from 0 to t_1, the drop-off rate (v) of the EAB curve is too small to be discernible, which has been shown by the rhombuses in Figure 2. These periods of time are also plotted by the dotted lines in Figure 6 according to the column of ($t_1 - 0$) in Table 3. When the content of the antioxidant is between c_2 and c_3 in Figure 1 (a), or between t_1 and t_2,

the v is the same to the v used to plot the dashed line in Figure 2, or the value of v_2 in Table 1. These curves are plotted by the dashed lines based on equation (9) in Figure 6. Equation (9) is the combination of equation (2) and equation (3).

$$\delta \cong 1 - \left(1 - e^{-v_2(t - t_1)}\right)^{(1/3)} \tag{9}$$

where $t_2 \geqq t > t_1$

When the content of the antioxidant is lower than c_3 shown in Figure 1 (a), or $t > t_2$, it means v should increase from v_2 to v_1 listed in Table 1 due to the deficiency of the antioxidant. The solid lines in Figure 6 are plotted by equation (10); they represent the EAB when aging time is longer than t_2. The curly bracket in equation (10) is the accumulated degradation ratio (V_d) from the beginning of the thermal aging. V_{d2} is the degradation ratio at t_2, or at the end of the dashed lines in Figure 6.

$$\delta \cong 1 - \left\{V_{d2} + (1 - V_{d2}) \cdot \left[1 - e^{-v_1(t - t_2)}\right]\right\}^{(1/3)} \tag{10}$$

where $t > t_2$, and

$$V_{d2} = 1 - e^{-v_2(t_2 - t_1)} \tag{11}$$

The EAB of the fresh XLPE insulation is about 500% [6]. The acceptable minimum EAB for the application in power plants is suggested to be 50% [16, 17]. Therefore, the normalized EAB (δ) is equal to (50% ÷ 500% = 0.1), which is represented by the chained line in Figure 6. The intersections of the solid lines and the chained line show the time to failure of the cable insulation in a probabilistic form.
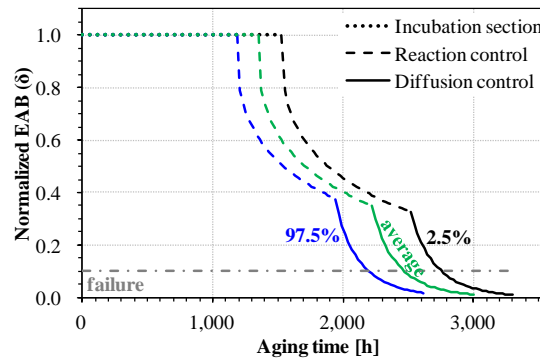

Figure 6. Multi-sectioned degradation curves of the EAB

4. DISCUSSION

The drop-off rate (v) is measured by the degradation of the EAB. It is similar but not the same to the degradation rate of chemical reactions. Hence, the incubation section in Figure 6 means negligible drop-off rate of the EAB curve rather than no chemical reaction in the insulation. In the paper [6], v is significantly affected by the content of the antioxidant left in the XLPE. When the content of the antioxidant is high, the bottleneck of the oxidation reaction is at the interface between oxygen and the polymer. In other words, the antioxidant can lower the reaction possibility. Therefore, the oxidation is reaction control. This is the condition before t_1, and the period between t_2 and t_1. After t_2, 98% of the antioxidant has drained off, oxidation can easier occur at the interface. As a result, the critical step for the reaction to succeed should be determined by the migration speed of the oxygen diffusing in the insulation, which is referred to diffusion control.

To draw the boundary between reaction- and diffusion-controlled oxidation, the depletion progress of the antioxidant should be studied. The experimental data in Figure 7 are the same to those in Figure 3. One paper suggested the depletion against time is linear [6]. To test this assumption, the linear fit for the experimental data in Figure 7 is represented by equation (12) since the z value, or the normalized content of the antioxidant, must be one when time (t) is zero. Similar to the equations from (5) to (8),

equation (13) to (16) have been developed to applied Bayesian Parameter Estimation. The priors, (-m) and σ, are assumed to be uniform distribution between 0.0006-0.0013 and 0-0.35, respectively. The results of (-m) and σ calculated by Bayesian Parameter Estimation are plotted by the PDFs in Figure 8 and Figure 9. The percentile of several (-m) values is listed in Table 4 and plotted in Figure 7. Corresponding to each (-m) value, the time required to reach a specific z value can be calculated by equation (12). The result is listed in Table 5.
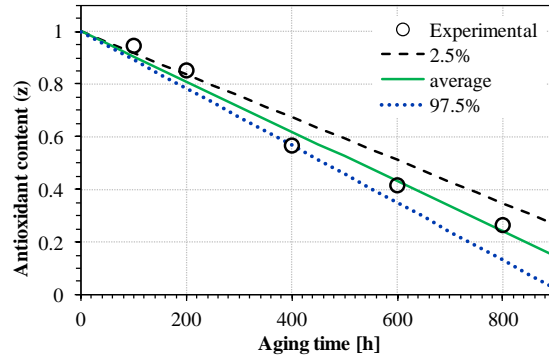

Figure 7. Comparison between experimental (the circles) and linearly-modeled (the lines) antioxidant content

$$z = m \cdot t + 1 \tag{12}$$

$$z_i \sim \mathcal{N}(\mu_z, \sigma) \tag{13}$$

$$\Pr(z_i \mid \mu_z, \sigma) = \frac{1}{\sqrt{2\pi\sigma^2}} \exp\left(-\frac{(z_i - \mu_z)^2}{2\sigma^2}\right) \tag{14}$$

$$\mu_z = m \cdot t + 1 \tag{15}$$

$$\Pr(z_i, t_i \mid m, \sigma) = \frac{1}{\sqrt{2\pi\sigma^2}} \exp\left(-\frac{[z_i - (m \cdot t + 1)]^2}{2\sigma^2}\right) \tag{16}$$
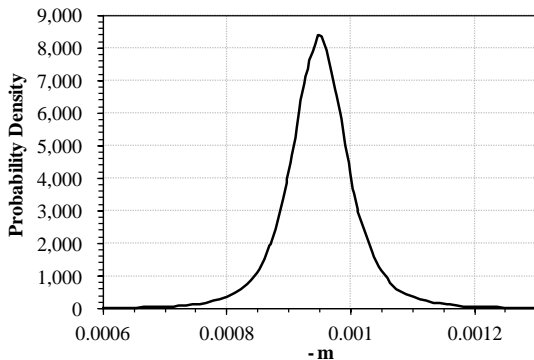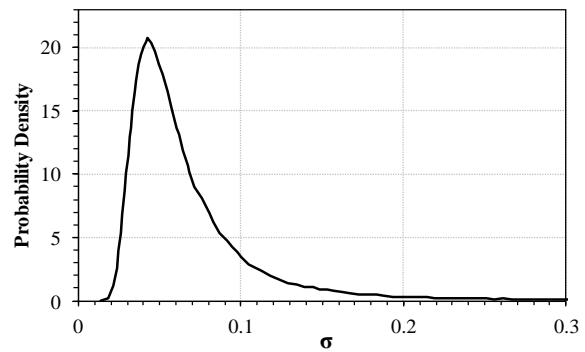

Figure 8. PDF of (-m)

Figure 9. PDF of the standard deviation

Table 4. The result of Bayesian parameter estimation

Percentile	(-m)
2.5	0.0008152
25	0.0009159
50*	0.0009492
75	0.0009829
97.5	0.001085

*The average of (-m) is 0.0009494.

Table 5. The content of the antioxidant (y) vs. aging time (p_i) [hours]

Percentile of (-m)	(p_1 - 0) z = 0.1	(p_2 - 0) z = 0	(p_2) - (p_1)
2.5	1,104	1,227	123
Average	948	1,053	105
97.5	829	922	92

Figure 7 models the depletion of the antioxidant by a linear function while Figure 3 represents the depletion by an exponential function. Figure 10 compares the experimental data with the averages plotted by the linear and exponential functions. When aging time in Figure 10 is shorter than 800 hours, two fitting functions both represent the experimental data well. However, the linear and exponential functions respectively predict y = 0.05 at point g and point h, indicating for the long-term prediction, the difference between the two functions is significant. We provide two reasons to state that the exponential fitting is more pertinent for long-term prediction:

First, the depletion may be caused by the decomposition or the diffusion of the antioxidant. The rate of either process subsides as time elapses, which means the slope should decreases when aging time increases. It shall be similar to the trend of the solid line instead of the dashed line in Figure 10.

Second, the values in the fourth column of Table 5 suggest that the linear fitting in Figure 10 may be not proper for the long-term prediction. The column shows the time required for the antioxidant content to decrease from 0.1 to ~0 should be less than 123 hours. However, in Figure 2, compared to the trend of 1A specimen possessing zero antioxidant, the curve of 2A specimen having 0.1 phr antioxidant does not plump for 800 hours. This means the antioxidant may not decrease from 0.1 phr to ~0 phr in 123 hours. In other words, the (p_2 - p_1) predicted by equation (12) listed in Table 5 is too short according to Figure 2.
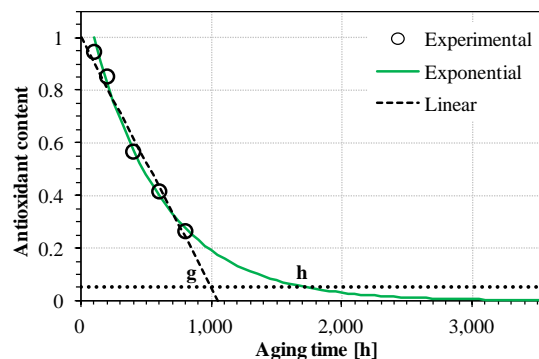

Figure 10. Comparison between the linear and exponential models

5. CONCLUSION

The degradation of cable insulation is a safety concern to power plants. Oxidation is a major reaction causing the degradation quantified by the EAB. The antioxidant is added to the insulation to slow down the oxidation, but its content decreases while aging. The content significantly affects the drop-off rate of the EAB. A multi-sectioned EAB curve can be plotted with respect to different drop-off rates based on the level of the antioxidant left in the insulation.

To model the depletion rate of the antioxidant, an exponential function serving as the likelihood of Bayesian Parameter Estimation has been developed. This probabilistic approach is first applied in the related research domain. It can represent the depletion rate with uncertainty to define the reliability of the insulation. Compared to the linear approximation for the depletion process of the antioxidant in the previous work [6], the proposed exponential model may be more pertinent to the long-term prediction according to the experimental data of the EAB.

Acknowledgements

References

[1] K. T. Gillen and R. L. Clough, "Time-temperature-dose rate superposition: a methodology for extrapolating accelerated radiation aging data to low dose rate conditions," *Polymer Degradation and Stability,* vol. 24, pp. 137-168, 1989.

[2] T. Šarac, N. Quiévy, A. Gusarov, and M. Konstantinović, "Influence of γ-irradiation and temperature on the mechanical properties of EPDM cable insulation," *Radiation Physics and Chemistry,* vol. 125, pp. 151-155, 2016.

[3] T. Yamamoto and T. Minakawa, "The final report of the project of assessment of cable aging for nuclear power plants," Japan Nuclear Energy Safety Organization, Tokyo, Japan JNES-SS-0903, July 2009.

[4] T. Seguchi, K. Tamura, A. Shimada, M. Sugimoto, and H. Kudoh, "Mechanism of antioxidant interaction on polymer oxidation by thermal and radiation ageing," *Radiation Physics and Chemistry,* vol. 81, pp. 1747-1751, 2012.

[5] T. Seguchi, K. Tamura, T. Ohshima, A. Shimada, and H. Kudoh, "Degradation mechanisms of cable insulation materials during radiation–thermal ageing in radiation environment," *Radiation Physics and Chemistry,* vol. 80, pp. 268-273, 2011.

[6] A. Shimada, M. Sugimoto, H. Kudoh, K. Tamura, and T. Seguchi, "Degradation distribution in insulation materials of cables by accelerated thermal and radiation ageing," *IEEE Transactions on Dielectrics and Electrical Insulation,* vol. 20, pp. 2107-2116, 2013.

[7] T. Seguchi, K. Tamura, H. Kudoh, A. Shimada, and M. Sugimoto, "Degradation of cable insulation material by accelerated thermal radiation combined ageing," *IEEE Transactions on Dielectrics and Electrical Insulation,* vol. 22, pp. 3197-3206, 2015.

[8] Y.-S. Chang and A. Mosleh, "Predictive model of the degradation of cable insulation subject to radiation and temperature," presented at the International Topical Meeting on Probabilistic Safety Assessment and Analysis (PSA), Pittsburgh, PA, 2017.

[9] Y.-S. Chang and A. Mosleh, "Physics-Based Model of the Degradation of Cable Insulation Subject to Radiation and Heat," presented at the IEEE Conference on Electrical Insulation and Dielectric Phenomenon, Fort Worth, TX, 2017.

[10] Y.-S. Chang and A. Mosleh, "Probabilistic Degradation Models for Cable Insulation in Nuclear Power Plants," presented at the ANS Winter Meeting and Nuclear Technology Expo, Washington, D.C., 2017.

[11] E. Rabiei, H. Chien, M. White, A. Mosleh, S. Iyer, and J. Woo, "Component Reliability Modeling Through the Use of Bayesian Networks and Applied Physics-based Models," in *Reliability and Maintainability Symposium (RAMS)*, Reno, Nevada, USA, 2018.

[12] E. Rabiei, E. L. Droguett, and M. Modarres, "A prognostics approach based on the evolution of damage precursors using dynamic Bayesian networks," *Advances in Mechanical Engineering,* vol. 8, p. 1687814016666747, 2016.

[13] E. Rabiei, E. L. Droguett, and M. Modarres, "Damage monitoring and prognostics in composites via dynamic Bayesian networks," in *Reliability and Maintainability Symposium (RAMS), 2017 Annual*, 2017, pp. 1-7.

[14] E. Rabiei, E. L. Droguett, and M. Modarres, "Fully Adaptive Particle Filtering Algorithm for Damage Diagnosis and Prognosis," *Entropy,* vol. 20, p. 100, 2018.

[15] E. Rabiei, E. L. Droguett, M. Modarres, and M. Amiri, "Damage precursor based structural health monitoring and damage prognosis framework," *Safety and Reliability of Complex Engineered Systems, vol,* pp. 2441-2449, 2015.

[16] IAEA, "Assessment and management of ageing of major nuclear power plant components important to safety: In-containment instrumentation and control cables Volume I," International Atomic Energy Agency, Vienna, Austria IAEA-TECDOC-1188, December 2000.

[17] EPRI and G. Toman, "Initial Acceptance Criteria Concepts and Data for Assessing Longevity of Low-Voltage Cable Insulations and Jackets," Electric Power Research Institute, Charlotte, North Carolina 1008211, March 2005.